Identification of novel quaternary domain interactions in the Hsp90 chaperone, GRP94

FEIXIA CHU,[1,2] JASON C. MAYNARD,[3] GABRIELA CHIOSIS,[4]
CHRISTOPHER V. NICCHITTA,[3] AND ALMA L. BURLINGAME[1,2]

[1]Mass Spectrometry Facility and [2]Department of Pharmaceutical Chemistry, University of California, San Francisco, California 94143, USA
[3]Department of Cell Biology, Duke University Medical Center, Durham, North Carolina 27710, USA
[4]Program in Molecular Pharmacology & Chemistry and Department of Medicine, Memorial Sloan-Kettering Cancer Center, New York, New York 10021, USA

Abstract

The structural basis for the coupling of ATP binding and hydrolysis to chaperone activity remains a central question in Hsp90 biology. By analogy to MutL, ATP binding to Hsp90 is thought to promote intramolecular N-terminal dimerization, yielding a molecular clamp functioning in substrate protein activation. Though observed in studies with recombinant domains, whether such quaternary states are present in native Hsp90s is unknown. In this study, native subunit interactions in GRP94, the endoplasmic reticulum Hsp90, were analyzed using chemical cross-linking in conjunction with tandem mass spectrometry. We report the identification of two distinct intermolecular interaction sites. Consistent with previous studies, one site comprises the C-terminal dimerization domain. The remaining site represents a novel intermolecular contact between the N-terminal and middle (M) domains of opposing subunits. This N+M domain interaction was present in the nucleotide-empty, ADP-, ATP-, or geldanamycin-bound states and could be selectively disrupted upon addition of synthetic geldanamycin dimers. These results identify a compact, intertwined quaternary conformation of native GRP94 and suggest that intersubunit N+M interactions are integral to the structural biology of Hsp90.

Keywords: adenosine nucleotides; geldanamycin; GRP94; Hsp90; molecular chaperone

Supplemental material: see www.proteinscience.org

Heat shock protein 90 (Hsp90) proteins comprise an essential, highly conserved, and ubiquitously expressed protein family, present in all protein-folding compartments of eubacteria and eukaryotes (Borkovich et al. 1989; Csermely et al. 1998; Picard 2002). Cytosolic Hsp90 function is critical to regulating the activity, turnover, and trafficking of a large number of proteins involved in signal transduction, cell cycle control, and steroid hormone responses (Richter and Buchner 2001; Pratt and Toft 2003; Prodromou and Pearl 2003; Wegele et al. 2004; Whitesell and Lindquist 2005). Although the precise chaperone function varies with the nature of its substrates, Hsp90 is thought to either stabilize its client proteins, and thereby prevent their proteasome-mediated degradation, and/or maintain client proteins in conformational states suitable for subsequent activation (Richter and Buchner 2001; Pratt and Toft 2003; Wegele et al. 2004; Cowen and Lindquist 2005; Whitesell and Lindquist 2005; Zhao et al. 2005). Glucose-regulated

protein of 94 kDa (GRP94), also known as gp96 or endoplasmin, is the ER paralog of Hsp90 and is found only in higher eukaryotes. GRP94 is essential for the proper assembly and maturation of numerous client proteins, including Toll-like receptors, a subset of integrins, and immunoglobulins (Melnick et al. 1992, 1994; Nigam et al. 1994; Muresan and Arvan 1997; Randow and Seed 2001). At present, the molecular basis for client protein recognition by GRP94 and the regulatory biology of GRP94–client protein interactions are largely a mystery.

Hsp90, GRP94, and the bacterial Hsp90, HtpG (high-temperature protein G), share an identical domain organization consisting of an N-terminal domain, a middle domain, and a C-terminal dimerization domain, the latter of which establishes the homodimeric quaternary structure of Hsp90 family proteins (Wearsch and Nicchitta 1996; Csermely et al. 1998; Argon and Simen 1999). Currently, a number of high-resolution Hsp90 N-terminal and N+M (N-terminal plus middle) domain structures have been described (Prodromou et al. 1997a,b; Stebbins et al. 1997; Meyer et al. 2003; Harris et al. 2004; Huai et al. 2005). These structural data, combined with biochemical and genetic studies, have revealed that Hsp90 function is intimately coupled to a cycle of ATP binding and hydrolysis (Obermann et al. 1998; Panaretou et al. 1998; Grenert et al. 1999). The N-terminal domain constitutes the primary binding site for adenosine nucleotides and their ansamycin and macrolide antibiotic mimetics, geldanamycin and radicicol (Grenert et al. 1997; Prodromou et al. 1997a; Stebbins et al. 1997; Roe et al. 1999; Huai et al. 2005). The middle domain contributes to the formation of the exterior portion of the adenosine nucleotide binding pocket and is thought to contribute catalytic residues to the N-terminal ATPase, thereby identifying Hsp90 as a split ATPase (Meyer et al. 2003; Wegele et al. 2003; Huai et al. 2005). In addition, the Hsp90 middle domain serves as the interaction site for Aha1, an ATPase-activating cochaperone (Panaretou et al. 2002; Lotz et al. 2003; Meyer et al. 2004). Crystallographic data demonstrate that Aha1 binding elicits a conformational change in the middle domain, which positions a catalytic loop in the middle domain in near physical proximity with the γ-phosphate of ATP (Meyer et al. 2004).

The structures of Hsp90 family member N-terminal and middle domains identify them as members of the GHKL family of ATP-binding proteins (Dutta and Inouye 2000). By structural and mechanistic homology with the GHKL family members GyrB and MutL, current models of the Hsp90 chaperone cycle propose that client protein capture occurs via an N-terminal "molecular clamp," in a manner analogous to the DNA-binding functions of GyrB and MutL (Kunkel and Erie 2005). In this model, ATP binding to the N-terminal domain elicits a transient, intermonomeric N-terminal dimerization reaction, and it is this conformational state (molecular clamp) that favors client protein

binding (Chadli et al. 2000; Prodromou et al. 2000). The structure of the GRP94 N-terminal domain closely resembles that of the Hsp90 N-terminal domain (Soldano et al. 2003). However, mammalian GRP94s contain a highly conserved 5–amino acid insertion in the nucleotide-binding domain that confers a ligand-binding selectivity and conformational response to ATP/ADP binding that differs substantially from that displayed by Hsp90 (Rosser and Nicchitta 2000; Soldano et al. 2003). In particular, comparisons of the molecular conformation of the ATP- or ADP-bound forms of Hsp90 and GRP94 demonstrate that adenosine nucleotide binding to GRP94 elicits a substantial displacement of the helix 1,4,5 domain, to yield an "open" lid conformation (Immormino et al. 2004; Dollins et al. 2005); in the paired Hsp90 action model (though not observed experimentally), ATP/ADP binding yields lid closure (Prodromou et al. 2000; Meyer et al. 2003). Nonetheless, the conformational change accompanying ATP/ADP binding to GRP94 exposes an interactive surface sufficient for dimerization of recombinant GRP94 N-terminal domain in vitro (Immormino et al. 2004). Interestingly, HtpG displays a conformational response to ADP binding mirroring, though to a less dramatic extent, that reported for GRP94; the proposed Hsp90 N-terminal dimerization interface was not, however, observed in the HtpG N+M domain crystal structures (Huai et al. 2005). In view of these similarities and differences, it remains an open question whether the ATP-driven "molecular clamp" conformation reported for yeast Hsp90 represents a unifying structural model for Hsp90 chaperone function (McLaughlin et al. 2004). The paucity of structural information on native, dimeric Hsp90 proteins has hampered resolution of this question.

In this study, we used a combined chemical cross-linking/ mass spectrometry experimental approach to define the subunit interface of native, full-length GRP94. Among the methods used to study protein–protein interactions, strategies based on chemical cross-linking have the potential to covalently capture transient interactions and conformations and have proven especially useful for dynamic systems (Back et al. 2003; Sinz 2003). Identification of the cross-linked amino acid residues provides valuable spatial restraints that can be employed to identify protein fold structures (Young et al. 2000; Dihazi and Sinz 2003), connectivity of secondary structures (Doyle et al. 1998; Cohen and Chait 2001), and, of relevance to the current study, protein interaction surfaces (Person et al. 2001; D'Ambrosio et al. 2003; Kopp et al. 2003; Lanman et al. 2003; Chu et al. 2004). We probed the dimeric interface of GRP94 using disuccinimidyl suberate (DSS), a homobifunctional N-hydroxysuccinimide (NHS) ester cross-linking reagent. Six intermonomeric cross-linked peptides were detected, and the cross-linked residues were unambiguously identified by tandem mass spectrometry. Two of the cross-links locate around the C-terminal dimerization domain of the protein. The remaining four

cross-links identify a dynamic, intermonomeric *trans*-proximity of N-terminal and middle domains of opposing subunits. This novel interface was observed in the nucleotide-empty as well as nucleotide-bound state of GRP94 yet was selectively lost upon addition of the synthetic geldanamycin dimer GMD-4c, which acts as a molecular "wedge" to constrain the relative steric orientation of the two subunits. These findings provide novel insights into the domain organization of GRP94, identify a potential mechanism for the previously reported negative cooperativity in adenosine ligand binding to the GRP94 N-terminal domain, and suggest additional modes of domain–domain interactions for Hsp90 chaperones.

Results

Cross-linking of GRP94 and differential LC-MS analysis

The cross-linking and mass spectrometric analysis strategy employed to map the native GRP94 dimeric interface is schematically illustrated in Figure 1. The noncovalent homodimeric nature of native GRP94 requires an
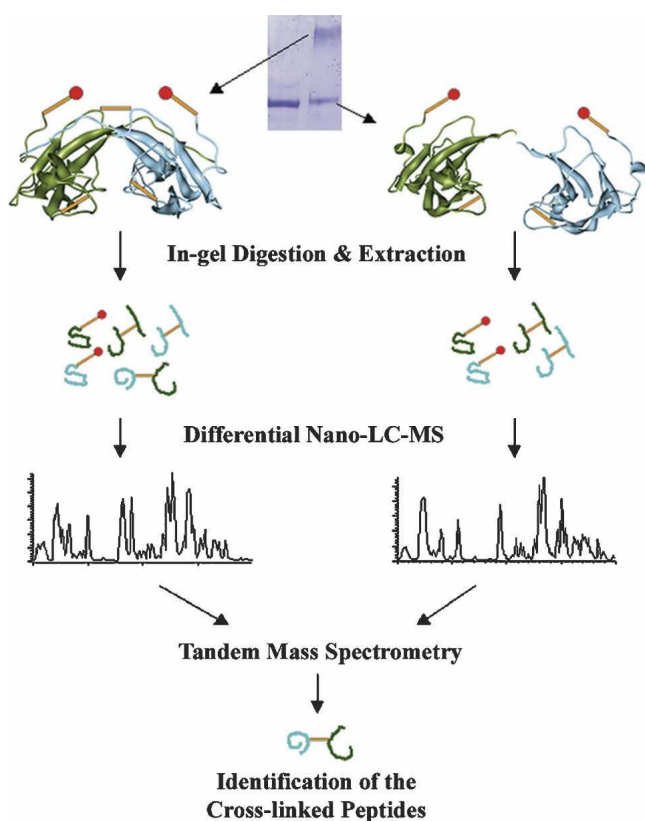

Figure 1. Differential nano-LC-MS analysis strategy to identify intermonomeric cross-linked species from homodimeric protein assemblies. Two polypeptide chains of the dimer complex are colored in green and in blue to distinguish their origin. (Orange sticks) Cross-linking bridges, (sticks with red dots) single-ended cross-links.

additional monomer/dimer separation step prior to the structural analysis, so that intermonomeric and intra-monomeric cross-linked species can be unambiguously distinguished. To achieve this goal, the cross-linking reaction products were separated by SDS-PAGE and in-gel proteolytic digestion mixtures of the well-resolved dimer and monomer bands were then analyzed by liquid chromatography mass spectrometry (LC-MS) (Fig. 1). By this methodology, intramonomeric cross-linking products, expected to be present in both the monomer and cross-linked dimer products, can be distinguished from intermonomeric cross-linking products, which will be solely present in the cross-linked dimer band, by subtractive LC-MS.

Near-neighbor subunit interactions were probed with DSS, which reacts with protein N-terminal α-amino and lysine ε-amino groups. In addition to the desired intermonomeric cross-linking reactions at the subunit–subunit protein interaction surfaces, DSS can also cross-link lysines within one monomer to give intramonomeric cross-links, or modify surface lysine residues, with the second reactive functionality being hydrolyzed to yield the surface adducts. These modifications slightly reduce the mobility of the monomeric fraction of the protein in reductive, denaturing gel electrophoresis (Fig. 2A). Under the reaction conditions employed in our studies, the covalently linked dimer band is the only higher molecular weight cross-linked form observed. In addition, studies performed at twofold lower or higher GRP94 concentrations, at an identical cross-linker/GRP94 ratio, give similar cross-linking yields, indicating that the reaction is specifically confined to GRP94 homodimers and not higher-order oligomeric cross-linking between GRP94 dimers (data not shown).

Identification of the C-terminal dimerization domain interface

To facilitate the detection of low stoichiometry cross-linked peptides and to increase the confidence in the identification of intermonomeric cross-linked species, we employed on-line capillary HPLC with nano-electrospray ionization (ESI) mass spectrometry for analysis of the tryptic digests. The total ion chromatograms (TIC) of the tryptic peptide mixtures from the cross-linked dimer (Fig. 2B) and the monomer (Fig. 2C) resemble each other, yet a closer comparison of the peptide elution profiles reveals significant differences. For example, among the peptides that elute at ~21 min from the reverse-phase capillary column, a peptide at m/z 664.34^{4+} is present only in the digest of the cross-linked dimer (insets, Fig. 2B,C). The identities of the two cross-linked peptide moieties comprising this peptide at m/z 664.34^{4+} are conclusively assigned by two continuous C-terminal fragment ion ladders (y_i and y_i') in the tandem mass spectrum (Fig. 3). The masses of
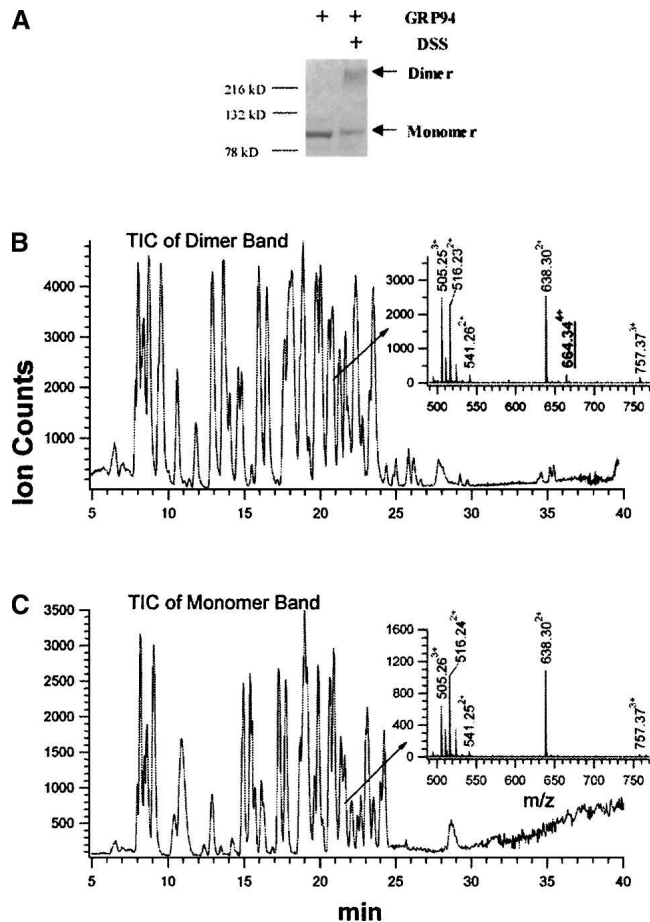
Figure 2. Cross-linking of the GRP94 dimer complex. (*A*) SDS-PAGE analysis of the cross-linking reaction. (*B,C*) Total ion chromatograms (TIC) of the tryptic digestion mixture of the cross-linked dimer band (*B*) and the monomer band (*C*). (*Insets*) Mass spectra of the peptides eluted at ~21 min.

the C-terminal sequence ions ($y_{1'}$ to $y_{10'}$) of the Lys547–Arg557 moiety match the anticipated values of the unmodified peptide, suggesting that the ε-amino group of Lys547 is the cross-linked site. Similarly, the masses of the C-terminal sequence ions (y_1 to y_8) of the Ile661–Lys671 moiety are the anticipated values, showing that all residues at the C terminus of Lys663 are unmodified. The mass of the first N-terminal sequence ion (i.e., b_2) from the same peptide moiety indicates that the first two N-terminal residues of this peptides are unmodified. Therefore, Lys663 is unambiguously assigned as the cross-linked site. The results from tandem mass spectrometry/differential LC-MS analysis thus establish that the ε-amino groups of Lys663 and Lys547 are cross-linked in an intermonomeric manner at the C-terminal homodimeric interface of GRP94.

The identity and structure of another intermonomeric cross-link observed with a m/z of 512.77⁴⁺ is determined by tandem mass spectrometry in an identical fashion (Table

1; Supplemental Material). This species corresponds to a cross-link between Lys630 and Lys547. The position of the three residues involved in these two cross-links is consistent with existing biophysical and crystallographic data (Wearsch and Nicchitta 1996; Harris et al. 2004). Both Lys630 and Lys663 reside in the C-terminal dimerization domain, with Lys663 corresponding to HtpG Ala555 on the helix 2 adjacent to the "jaws" of the HtpG C-terminal homodimer (Harris et al. 2004). Lys547 corresponds to yeast Hsp90 Lys480 on helix 13 of the Hsp90 N+M domain, adjacent to the C terminus of the middle domain (Huai et al. 2005). These data indicate that regions of GRP94 near the N-terminal region of the C-terminal dimerization domain reside in close intermolecular proximity to regions near the C-terminal region of the middle domain, which is in good agreement with previous bacterial two-hybrid system studies (Yamada et al. 2003). On a broader level, the data presented above demonstrate that differential LC-MS analysis used in conjunction with tandem mass spectrometry provides a robust and reliable approach to identify intermonomeric cross-linked species for protein complexes that contain multiple copies of the same polypeptide chains.
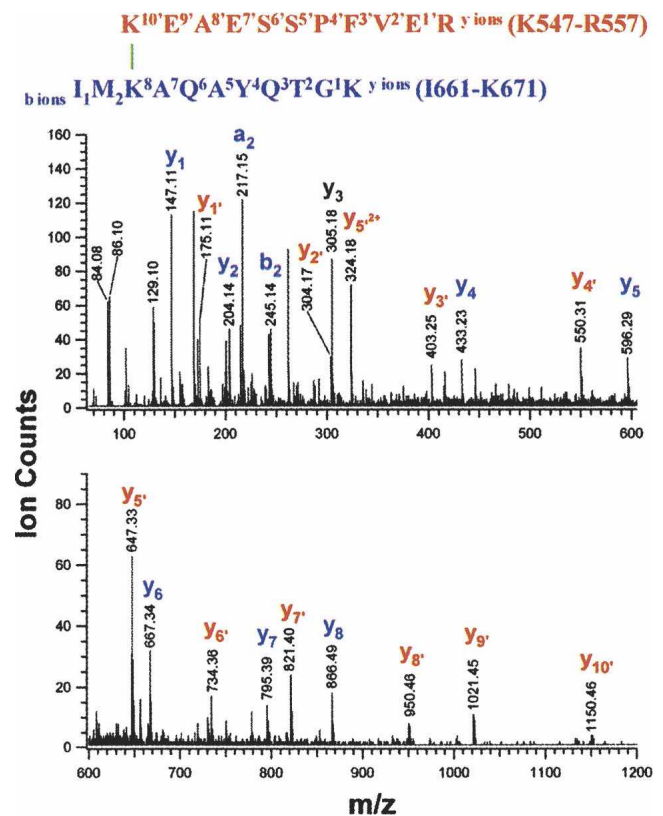
Figure 3. Structure and low-energy CID spectrum of the cross-linked species with a m/z value of 664.34⁴⁺ from the GRP94 dimer digest. C-terminal sequence ions that did not contain the cross-linker moiety were labeled in lowercase letters, e.g., y_i (blue), and $y_{i'}$ (red) ions.

Table 1. *Intermonomeric cross-linked species identified by differential nano-LC-MS and tandem mass spectrometry*

Exp. m/z	Δ (ppm)	Cross-linked residues	Peptide sequences
664.3417[4+]	6.3	K663–K547	I661–K671
		(K594–K480)[a]	K547–R557
512.7652[4+]	2.7	K630–K547	D629–K633
		(Q561–K480)[a]	K547–R557
432.5076[4+]	−0.9	K462–K161	K462–K463
		(K394–N91)[a]	E157–K168
549.0895[4+]	−0.3	K458–K161	L456–R461
		(K390–N91)[a]	E157–K168
584.7225[5+]	−1.0	K455–K114	E449–K458
		(K387–K44)[a]	E103–K116
606.6124[4+]	11	K458–K114	L456–R461
		(K390–K44)[a]	E103–K116

[a] The cross-linked residues in the GRP94 dimeric complex were mapped back onto the corresponding yeast Hsp90 as indicated in parentheses.

Identification of novel N-terminal and middle domain interactions

In addition to two pairs of cross-links abutting the C-terminal dimerization domain, we observed four distinct intermonomeric cross-links, involving residues from the N-terminal and middle domains (Table 1). Comparison of the extracted ion chromatograms (XIC) for m/z 549.09 ions observed during the LC runs of dimer and momomer digests demonstrates the unique presence of the m/z 549.09 ion in the LC run of the dimer digest (Fig. 4A,B). Thus, in the peptide cohort eluting at ~27.8 min, a peptide with m/z 549.09[4+] exists only in cross-linked dimer digest (insets, Fig. 4A,B). Interpretation of the low-energy collision-induced-dissociation (CID) spectrum (Fig. 5) obtained for this component reveals that it is composed of two cross-linked peptide moieties, Leu456–Arg461, derived from the middle domain, and Glu157–Lys168, derived from the N-terminal domain. The masses of the C-terminal sequence ion series of Glu157–Lys168 moiety up to Lys161 (i.e., y_1 to y_7) as well as the masses of the N-terminal sequence ion series up to Lys161 (i.e., b_2 to b_4) appear unmodified. Thus, Lys161 can be assigned conclusively as the cross-linked site. Similarly, Lys458 is assigned as the other cross-linked site. Therefore, we conclude that Lys161 resides in close apposition to Lys458 and represents a GRP94 near-neighbor interaction site/interface. The identities and structures of three other intermonomeric N+M domain cross-linked species were determined by differential LC-MS and tandem mass spectrometry in the identical fashion (Table 1; Supplemental Material). Combined, these data identify a novel GRP94 N+M domain intersubunit interaction site and distinguish the domain–domain interactions occurring in GRP94 from those seen with Hsp90. For Hsp90, the primary N-terminal and middle domain interactions site(s) are thought to be intramonomeric, with interactions between

monomer N+M domains functioning to orient potential ATPase catalytic residues on the middle domain with N-terminal-domain-bound ATP (Meyer et al. 2003). In contrast, crystal forms of the HtpG N+M domain contain two different dimer forms with dimerization reflecting intersubunit interactions between opposing N+M domains (Huai et al. 2005). However, none of the dimer forms would be expected to yield the intermonomeric cross-links described above. It remains to be determined whether the N+M domain intersubunit interactions observed with native GRP94 resemble those reported by D. Agard (Jackson et al. 2004).

Ligand modulation of the GRP94 intermonomeric N+M domain interface

Current structural models of nucleotide-empty forms of Hsp90 identify an intramonomeric interaction between the N-terminal and middle domains (yeast Hsp90) (Meyer et al. 2003), or an antiparallel dimeric orientation yielding an intermolecular N+M domain interface (HtpG) (Huai et al. 2005). For the nucleotide-liganded form of Hsp90, the ATP-bound form yields the N-terminal domain "molecular clamp" (Chadli et al. 2000; Prodromou et al. 2000), whereas for recombinant (1–559) HtpG, an antiparallel intermonomeric middle and middle domain interface was observed (Huai et al. 2005). Our cross-linking
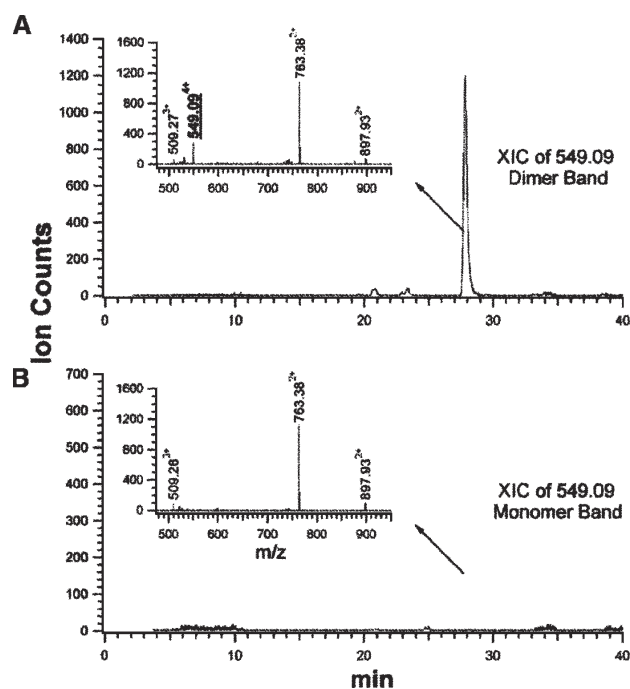
Figure 4. The intermonomeric cross-linked species with a m/z value of 549.09[4+] were identified only in the covalently linked dimer digest. (*A,B*) Extract ion chromatograms (XIC) of m/z value 549.09 from the tryptic digestion mixture of the dimer band (*A*) and the monomer band (*B*). (*Insets*) Mass spectra of the peptides eluted at ~27.8 min.
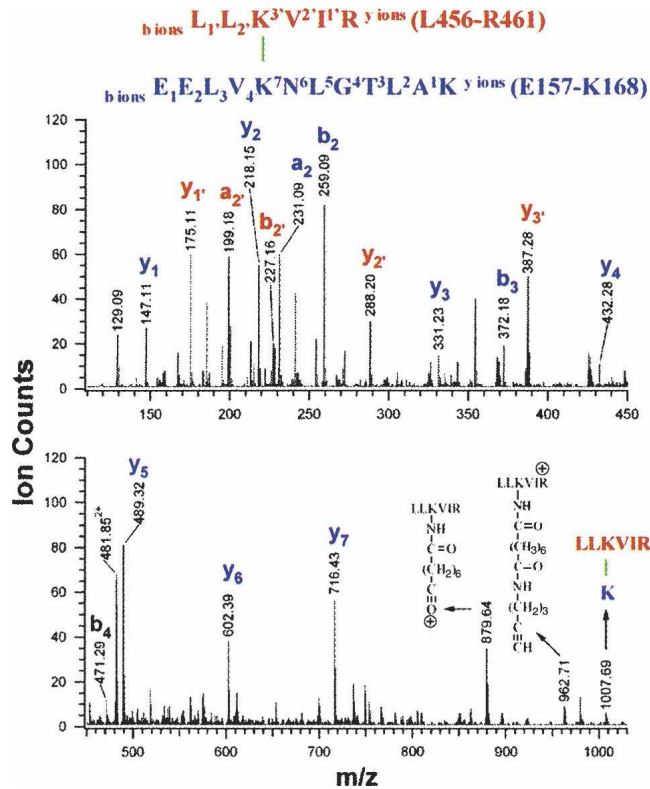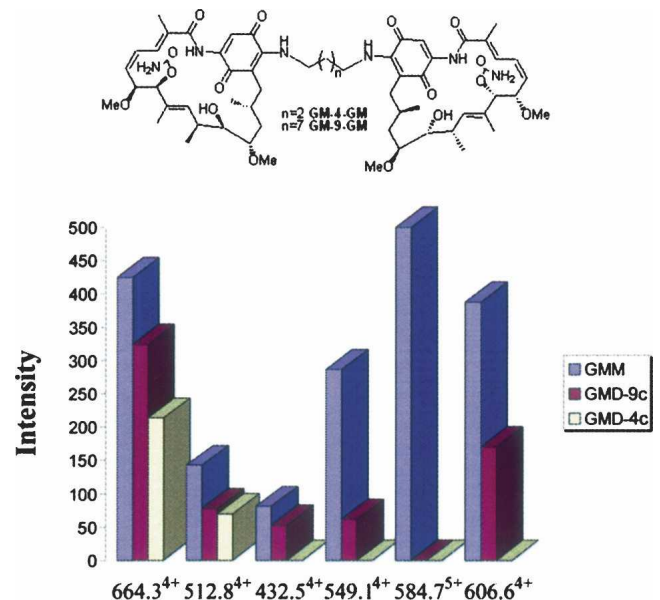
Figure 5. Structure and low-energy CID spectrum of the cross-linked species with a m/z value of 549.09^{4+} from the GRP94 dimer digest. C-terminal sequence ions that did not contain the cross-linker moiety were labeled in lowercase letters, e.g., y_i (blue), and y_i' (red) ions.

4c and GMD-9c are bivalent geldanamycin molecules, covalently tethered four- or nine-carbon linkers, respectively (Chiosis et al. 2006). We reason that if the GRP94 intermolecular N+M domain interface is dynamically sampled, a bivalent N-terminal ligand could act as a molecular ''wedge'' and thereby reduce or eliminate the intermolecular N+M domain interaction.

The results of these experiments are summarized in Figure 6. As expected, the relative intermolecular cross-linking efficiencies occurring at the C-terminal dimerization domain were not dramatically altered in either the GRP94/GMD-4c or the GRP94/GMD-9c complexes, as compared with the GRP94/GM complex (Fig. 6, signals at m/z 664.3^{4+} and 512.8^{4+}). In contrast, none of the four intermonomeric cross-links on the N-terminal and middle domains were detected in the GRP94/GMD-4c complex (Fig. 6, signals at m/z 432.5^{4+}, 549.1^{4+}, 584.7^{4+}, and 606.6^{4+}). When native GRP94 was complexed with the geldanamycin dimer tethered by a long linker chain, i.e., GMD-9c, some of the cross-links surrounding the N+M domain interface were again detected, though at reduced abundance (Fig. 6). These results suggest that binding of GMD-4c complex to GRP94 introduces a steric constraint at the N+M domain interface, thus stabilizing an ''open,'' weakly intertwined, quaternary conformation. This steric constraint can be partially alleviated by an increase in the linker chain distance/ligand conformational flexibility, as observed in the GRP94/GMD-9c complex. These results

results indicate that in the ligand-empty state, native GRP94 assumes a quaternary orientation where the N-terminal and middle domains intertwine to yield a parallel intermolecular N+M domain interface. This intertwined quaternary conformation is distinct from that seen in the low-resolution density map of full-length HtpG dimer, which distally projects the middle and the N-terminal domain of each monomer from the intimately wrapped C-terminal dimerization domains (Harris et al. 2004). To date, we have not observed any changes in GRP94 quaternary structure upon binding of ATP or ADP (data not shown). It is thus likely that the GRP94 intermonomeric N+M domain interaction detected by our cross-linking studies represents a primary, dynamically sampled GRP94 conformational state. Consistent with this hypothesis, the observation that GRP94 displays negative cooperativity (half site reactivity) in adenosine ligand binding indicates that the ligand occupancy state of the two subunits is in dynamic communication (Hutchison et al. 1990; Rosser and Nicchitta 2000; Rosser et al. 2004). To further test this hypothesis, we extended our cross-linking studies to include GRP94 in complex with geldanamycin or either of the geldanamycin dimers, GMD-4c and GMD-9c. GMD-

Figure 6. Comparison of the amount of the intermonomeric cross-linked peptides of GRP94 in complex with geldanamycin, GMD-4c, or GMD-9c. The digestion mixtures of DSS cross-linked dimer were analyzed consecutively on LC-MS. The amount of the cross-linked peptides is represented by the peak intensity of the corresponding peptides.

best fit a model where the intertwined, intersubunit N+M domain interface is dynamically sampled by GRP94 and where imposition of steric hindrance at the N+M domain interface, e.g., binding of GMD-4c to the N-terminal adenosine nucleotide-binding site, shifts the equilibrium away from this conformation.

Discussion

Using a coupled chemical cross-linking/mass spectrometry experimental approach, we report a novel, intermonomeric N-terminal domain/middle domain interface in the ER Hsp90, GRP94. As well, we confirm prior identifications of an intermonomeric interface in the GRP94 C-terminal region functioning in subunit dimerization (Nemoto et al. 1996; Wearsch and Nicchitta 1996). Regulated N-terminal domain interactions figure prominently in current structural models of Hsp90 chaperone function (Prodromou et al. 2000; Wegele et al. 2003). In combining the study of native dimeric GRP94 with an experimental approach that distinguishes intra- versus intersubunit interactions, we now propose that GRP94 assumes an intertwined quaternary conformation that promotes the described N+M domain intersubunit interaction. This proposed conformational state, identified in native dimeric GRP94, shares with current models a focus on intersubunit interactions but differs in its emphasis on N-terminal domain/middle domain interactions as the primary intersubunit interaction site. This conformational state can be efficiently disrupted by bivalent N-terminal ligands, which, by coupling the two N-terminal ligand binding sites, limit the steric interactions necessary for assembly of the intersubunit N-terminal and middle domain interface. We propose that this newly identified interface serves as the structural basis for the previously reported negative cooperativity in adenosine ligand binding to GRP94 and suggest, by functional comparison with the DNA mismatch repair enzymes MutL and MutS, that similar quaternary interactions may occur in other members of the family of Hsp90 proteins (Hutchison and Fox 1989; Hutchison et al. 1990; Rosser and Nicchitta 2000).

An intertwined GRP94 conformation

Proteins and protein assemblies have been observed to simultaneously exist in populations of diverse conformations (Celikel et al. 2003; Dumas et al. 2003; James et al. 2003). Such dynamic structural interconversions provide the basis for the functional diversity of proteins and protein assemblies, yet are often difficult to capture. In utilizing an experimental approach that can trap transient structural intermediates, we have identified a novel domain interface in GRP94 that represents a *trans*-subunit interaction of N-terminal and middle domains. Recent crystallographic studies of the recombinant HtpG N+M domain have also identified *trans*-subunit N-terminal and

middle domain interactions, one an N-terminal and middle domain interaction prominent in the unliganded form and the other a middle and middle domain interaction occurring upon binding of ADP (Huai et al. 2005). Both dimer forms are established through an antiparallel orientation of the two subunits, which contrasts with current models in which parallel subunits function to allow regulated, transient interactions between two N-terminal domains (Prodromou et al. 2000; Wegele et al. 2003). As noted by Huai et al. (2005), it is not known if the antiparallel subunit orientation mirrors that occurring in the native HtpG dimer. In the current study, intersubunit domain–domain interactions were assayed with native dimeric GRP94, and in this setting, *trans* N-terminal and middle domain interactions are detected. The location of these intermonomeric cross-linked residues is not compatible, however, with the two antiparallel subunit orientations observed in HtpG N+M domain dimers. Therefore, it is likely that the C-terminal dimerization domain of Hsp90 chaperones serves key functions in directing/constraining interactions between the N-terminal and middle domains. That the C-terminal dimerization domain might function in such a manner is supported by high-resolution crystal structure models of the HtpG C-terminal domain, which depict a parallel projection of the two subunits (Harris et al. 2004).

Cross-linking studies on GRP94 in complex with geldanamycin, radicicol, or ATP/Mg^{2+} reveal that neither the dimer cross-linking yield, the position of cross-linked residues, nor the abundance of the cross-linked species in the ligand-bound protein is significantly different from those of the native *apo*-GRP94 protein (data not shown). We conclude, then, that the intersubunit GRP94 N+M domain interactions reported here cannot be attributed to transient, ATP-induced N-terminal domain dimerization, as suggested by the ''molecular clamp'' model (Chadli et al. 2000; Prodromou et al. 2000). The observed GRP94 *trans* N-terminal and middle domain interactions are of a transient, dynamic nature; constraining the conformational dynamics of the N-terminal domains, by addition of bivalent geldanamycin ligands, shifts the equilibrium away from this compact conformation without disrupting the primary C-terminal homodimeric interface. These results suggest that native GRP94 rapidly samples an ''open'' conformation, with the C-terminal dimerization domain as the only subunit–subunit interaction site, as well as an ''intertwined'' conformation, where the two monomers reside in close physical proximity to one another (Fig. 7).

Implications of the close, intertwined conformation on GRP94

We have established that four of the intermonomeric cross-linked species involve two residues, Lys161 and Lys114, on the GRP94 N-terminal domain and three
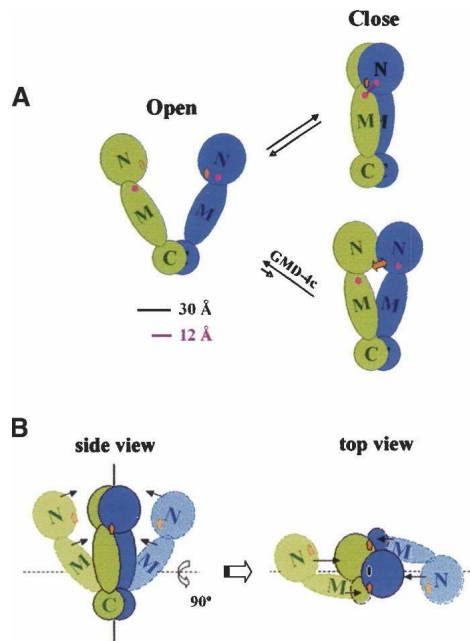
Figure 7. A model for GRP94 subunit interaction dynamics. GRP94 N-terminal, middle, and C-terminal domains are annotated as N, M, and C, respectively. (Orange squares) Adenosine nucleotide binding sites, (magenta circles) approximate positions for the clustered residues involved in N+M domain cross-linking reaction. The diameter of the C-terminal domain is ~30 Å, and the maximal distance the cross-linker (DSS) can span is 12 Å. (*A*) As illustrated, GRP94 samples both an "open" (Harris et al. 2004) and "closed" conformation, with intersubunit N+M domain cross-linking limited to the "closed" conformation. In this model, the two distinct conformers constitute a pre-existing conformational equilibrium, independent of adenosine nucleotide binding. The addition of bivalent geldanamycin ligand, GMD-4c (orange double arrow), introduces steric hindrance at the intersubunit N+M surface and thereby prevents the intersubunit cross-links between the N-terminal and middle domains. (*B*) Additional topological representations of the model depicted in *A*, emphasizing the intersubunit N+M interactions.

residues, Lys462, Lys458, and Lys455, on the GRP94 middle domain. Lys462, Lys458, and Lys455, corresponding to Lys394, Lys390, and Lys387, respectively, in yeast Hsp90, cluster at the beginning of elongated helix 2 of the middle domain. This domain has been proposed to function as a catalytic loop and was initially identified as being topologically equivalent to the requisite elements for ATPase activation in both GyrB and MutL (Meyer et al. 2003). In support of a functional role for N-terminal and middle domain interactions, yeast Hsp90 Arg380Ala and Gln384Ala mutants are not viable in vivo, and display compromised Hsp90 ATPase activity in vitro (Meyer et al. 2003). In the *Escherichia coli* HtpG N+M domain structure, however, the equivalent residues are too distant from the ATP-binding site to serve in the *cis*-enhancement of ATP hydrolysis (Huai et al. 2005). Nevertheless, our cross-linking results reveal a close proximity of the proposed middle domain "catalytic loop" to the ATP-

binding site in an intermonomeric manner, suggesting that Arg380Ala and Gln384Ala mutations possibly interfere either with this *trans* dimeric interaction on the N+M domains or assembly of the split ATPase.

Although GRP94 is an obligate homodimer, equilibrium and calorimetric binding studies demonstrate that GRP94 binds 1 mol of the N-terminal domain ligand N-ethylcarboxamidoadenosine (NECA) per mol of dimer (Hutchison et al. 1990; Rosser and Nicchitta 2000). The structural basis for such negative cooperativity remains to be determined; it is intriguing to consider that the intermonomeric N-terminal and middle domain interactions described in the current study function to communicate the ligand occupancy state of the two subunits, so as to create a functional asymmetry in the protein. Such a phenomenon would have a direct functional parallel with another member of the DNA repair enzyme family, MutS. MutS, like MutL, is a "split" ATPase and a dimer. For MutS of *E. coli*, human, and yeast, equilibrium binding of ADP occurs at a stoichiometry of 1 mol ADP per mol MutS dimer (Antony and Hingorani 2003; Bjornson and Modrich 2003; Martik et al. 2004). Thus MutS, like GRP94, displays functionally asymmetric binding of adenosine ligands, and available data strongly support the conclusion that MutL, the DNA mismatch repair GHKL family member, displays negative cooperativity in adenosine nucleotide binding (Kunkel and Erie 2005). Given that the asymmetry in adenosine nucleotide binding to MutS and MutL is conferred through intersubunit interactions, it is reasonable to consider that the intersubunit N-terminal and middle domain interactions identified in GRP94 act similarly to regulate the subunit stoichiometry of nucleotide binding to GRP94. Based on the existing structural homologies between MutL and Hsp90, we speculate that Hsp90 and HtpG display similar intersubunit N-terminal and middle domain interactions and that such interactions contribute to the regulation of the binding and hydrolysis of ATP. In this view, the N-terminal and middle domains of Hsp90 proteins would participate in three-dimensional domain swapping, a phenomenon known to contribute to subunit oligomerization and negative cooperativity (Di Donato et al. 1987; Liu et al. 2002). These and related models are currently under investigation.

Materials and methods

Materials

DSS was purchased from Pierce, and modified trypsin was obtained from Promega. GRP94 was purified from freshly isolated porcine pancreas as previously described (Rosser and Nicchitta 2000). Briefly, porcine pancreas rough microsomes (RM) were detergent permeabilized by addition of 10 mM CHAPS (3-[(3-cholamidopropyl)-dimethylammonio]-1-propane

sulfonate), and the detergent-treated RM suspension was centrifuged to yield a pellet fraction, containing endoplasmic reticulum membrane proteins, and a supernatant fraction, containing ER lumenal proteins. GRP94 was purified from the lumenal protein fraction by anion exchange (SourceQ, GE/Amersham Life Sciences) and gel filtration (Superdex 200, GE/Amersham Life Sciences) chromatography. The GRP94-containing fractions in the gel filtration step were pooled and concentrated by centrifugal ultrafiltration (Centricon-30, Amicon,). Protein purity was routinely >95%, as determined by Coomassie Blue–stained SDS-PAGE analysis.

Cross-linking reactions and in-gel tryptic digestion

Stock solutions of the cross-linking agent were prepared fresh at a concentration of 25 mM in DMSO. GRP94 (~150 pmol for each reaction, at 5 μM in 20 mM sodium phosphate buffer at pH 7.8) was incubated with a 20-fold molar excess of DSS in each cross-linking reaction. The reactions were carried out for 0.5 h at room temperature, quenched with 1.5 μL of 0.8 M ammonium hydroxide, and incubated for an additional 15 min at room temperature. The reaction mixtures were then concentrated under vacuum, mixed with sample buffer, boiled for 5 min, and loaded onto 4%–15% SDS-PAGE mini-gels (Bio-Rad). Protein bands were visualized with Coomassie brilliant blue. In-gel digestion on monomer and dimer bands was performed utilizing a procedure described at http://caravaggio.ucsf.edu/ingel.html. Typically, 5 μL (50 ng/μL) modified trypsin (porcine, side-chain protected; Promega) was used for each gel band, and digestions were carried out for 4 h at 37°C. Peptides were extracted from gel pieces with 30 μL of 50% acetonitrile/2% formic acid, and the acetonitrile/formic acid extract was reduced through evaporation to 20 μL before mass spectrometric analysis.

On-line capillary LC-MS and LC-MS-MS analysis of cross-linked peptides

A 1-μL aliquot of the digestion mixture was injected into an UltiMate capillary LC system via a FAMOS Autosampler (LC Packings), and separated by a 75-μm × 15-cm C18 reverse-phase capillary column at a flow rate of ~300 nL/min. The HPLC eluent was connected directly to the micro-ion electrospray source of a QSTAR Pulsar QqTOF mass spectrometer (Applied Biosystem/MDS Sciex). Typical performance characteristics were >8000 resolution with 30-ppm mass measurement accuracy in both MS and CID modes. LC-MS data were acquired using the Analyst QS software (Applied Biosystems). The centroided LC-MS data were then deisotoped and reconstructed to generate the peptide list for each LC-MS run. The lists of tryptic peptides extracted from the covalently linked GRP94 dimer band and the DSS-treated GRP94 monomer band were thoroughly compared to identify the peptides that were uniquely present in the digest of the cross-linked dimer species (Fig. 1). For those peptides uniquely recovered in the digest of the GRP94 cross-linked dimer, all possible cross-linking combinations were predicted by MS-Bridge, a program in the UCSF ProteinProspector package (http://prospector.ucsf.edu).

Acknowledgments

References

Antony, E. and Hingorani, M.M. 2003. Mismatch recognition-coupled stabilization of Msh2–Msh6 in an ATP-bound state at the initiation of DNA repair. *Biochemistry* **42:** 7682–7693.

Argon, Y. and Simen, B.B. 1999. GRP94, an ER chaperone with protein and peptide binding properties. *Semin. Cell Dev. Biol.* **10:** 495–505.

Back, J.W., de Jong, L., Muijsers, A.O., and de Koster, C.G. 2003. Chemical cross-linking and mass spectrometry for protein structural modeling. *J. Mol. Biol.* **331:** 303–313.

Bjornson, K.P. and Modrich, P. 2003. Differential and simultaneous adenosine di- and triphosphate binding by MutS. *J. Biol. Chem.* **278:** 18557–18562.

Borkovich, K.A., Farrelly, F.W., Finkelstein, D.B., Taulien, J., and Lindquist, S. 1989. hsp82 is an essential protein that is required in higher concentrations for growth of cells at higher temperatures. *Mol. Cell. Biol.* **9:** 3919–3930.

Celikel, R., McClintock, R.A., Roberts, J.R., Mendolicchio, G.L., Ware, J., Varughese, K.I., and Ruggeri, Z.M. 2003. Modulation of α-thrombin function by distinct interactions with platelet glycoprotein Ibα. *Science* **301:** 218–221.

Chadli, A., Bouhouche, I., Sullivan, W., Stensgard, B., McMahon, N., Catelli, M.G., and Toft, D.O. 2000. Dimerization and N-terminal domain proximity underlie the function of the molecular chaperone heat shock protein 90. *Proc. Natl. Acad. Sci.* **97:** 12524–12529.

Chiosis, G., Aguirre, J., and Nichitta, C.V. 2006. Synthesis of Hsp90 dimerization modulators. *Bioorg. Med. Chem. Lett.* (in press).

Chu, F., Shan, S.O., Moustakas, D.T., Alber, F., Egea, P.F., Stroud, R.M., Walter, P., and Burlingame, A.L. 2004. Unraveling the interface of signal recognition particle and its receptor by using chemical cross-linking and tandem mass spectrometry. *Proc. Natl. Acad. Sci.* **101:** 16454–16459.

Cohen, S.L. and Chait, B.T. 2001. Mass spectrometry as a tool for protein crystallography. *Annu. Rev. Biophys. Biomol. Struct.* **30:** 67–85.

Cowen, L.E. and Lindquist, S. 2005. Hsp90 potentiates the rapid evolution of new traits: Drug resistance in diverse fungi. *Science* **309:** 2185–2189.

Csermely, P., Schnaider, T., Soti, C., Prohaszka, Z., and Nardai, G. 1998. The 90-kDa molecular chaperone family: Structure, function, and clinical applications. A comprehensive review. *Pharmacol. Ther.* **79:** 129–168.

D'Ambrosio, C., Talamo, F., Vitale, R.M., Amodeo, P., Tell, G., Ferrara, L., and Scaloni, A. 2003. Probing the dimeric structure of porcine aminoacylase 1 by mass spectrometric and modeling procedures. *Biochemistry* **42:** 4430–4443.

Di Donato, A., Piccoli, R., and D'Alessio, G. 1987. Co-operativity in seminal ribonuclease function: Binding studies. *Biochem. J.* **241:** 435–440.

Dihazi, G.H. and Sinz, A. 2003. Mapping low-resolution three-dimensional protein structures using chemical cross-linking and Fourier transform ion-cyclotron resonance mass spectrometry. *Rapid Commun. Mass Spectrom.* **17:** 2005–2014.

Dollins, D.E., Immormino, R.M., and Gewirth, D.T. 2005. Structure of unliganded GRP94, the endoplasmic reticulum Hsp90. Basis for nucleotide-induced conformational change. *J. Biol. Chem.* **280:** 30438–30447.

Doyle, D.A., Morais Cabral, J., Pfuetzner, R.A., Kuo, A., Gulbis, J.M., Cohen, S.L., Chait, B.T., and MacKinnon, R. 1998. The structure of the potassium channel: Molecular basis of K+conduction and selectivity. *Science* **280:** 69–77.

Dumas, J.J., Kumar, R., Seehra, J., Somers, W.S., and Mosyak, L. 2003. Crystal structure of the GpIbα-thrombin complex essential for platelet aggregation. *Science* **301:** 222–226.

Dutta, R. and Inouye, M. 2000. GHKL, an emergent ATPase/kinase superfamily. *Trends Biochem. Sci.* **25:** 24–28.

Grenert, J.P., Sullivan, W.P., Fadden, P., Haystead, T.A., Clark, J., Mimnaugh, E., Krutzsch, H., Ochel, H.J., Schulte, T.W., Sausville, E., et al. 1997. The amino-terminal domain of heat shock protein 90 (hsp90) that binds geldanamycin is an ATP/ADP switch domain that regulates hsp90 conformation. *J. Biol. Chem.* **272:** 23843–23850.

Grenert, J.P., Johnson, B.D., and Toft, D.O. 1999. The importance of ATP binding and hydrolysis by hsp90 in formation and function of protein heterocomplexes. *J. Biol. Chem.* **274:** 17525–17533.

Harris, S.F., Shiau, A.K., and Agard, D.A. 2004. The crystal structure of the carboxy-terminal dimerization domain of htpG, the *Escherichia coli* Hsp90, reveals a potential substrate binding site. *Structure* **12:** 1087–1097.

Huai, Q., Wang, H., Liu, Y., Kim, H.Y., Toft, D., and Ke, H. 2005. Structures of the N-terminal and middle domains of *E. coli* Hsp90 and conformation changes upon ADP binding. *Structure* **13:** 579–590.

Hutchison, K.A. and Fox, I.H. 1989. Purification and characterization of the adenosine A2-like binding site from human placental membrane. *J. Biol. Chem.* **264:** 19898–19903.

Hutchison, K.A., Nevins, B., Perini, F., and Fox, I.H. 1990. Soluble and membrane-associated human low-affinity adenosine binding protein (adenotin): Properties and homology with mammalian and avian stress proteins. *Biochemistry* **29:** 5138–5144.

Immormino, R.M., Dollins, D.E., Shaffer, P.L., Soldano, K.L., Walker, M.A., and Gewirth, D.T. 2004. Ligand-induced conformational shift in the N-terminal domain of GRP94, an Hsp90 chaperone. *J. Biol. Chem.* **279:** 46162–46171.

Jackson, S.E., Queitsch, C., and Toft, D. 2004. Hsp90: From structure to phenotype. *Nat. Struct. Mol. Biol.* **11:** 1152–1155.

James, L.C., Roversi, P., and Tawfik, D.S. 2003. Antibody multispecificity mediated by conformational diversity. *Science* **299:** 1362–1367.

Kopp, D.A., Berg, E.A., Costello, C.E., and Lippard, S.J. 2003. Structural features of covalently cross-linked hydroxylase and reductase proteins of soluble methane monooxygenase as revealed by mass spectrometric analysis. *J. Biol. Chem.* **278:** 20939–20945.

Kunkel, T.A. and Erie, D.A. 2005. DNA mismatch repair. *Annu. Rev. Biochem.* **74:** 681–710.

Lanman, J., Lam, T.T., Barnes, S., Sakalian, M., Emmett, M.R., Marshall, A.G., and Prevelige Jr., P.E. 2003. Identification of novel interactions in HIV-1 capsid protein assembly by high-resolution mass spectrometry. *J. Mol. Biol.* **325:** 759–772.

Liu, Y., Gotte, G., Libonati, M., and Eisenberg, D. 2002. Structures of the two 3D domain-swapped RNase A trimers. *Protein Sci.* **11:** 371–380.

Lotz, G.P., Lin, H., Harst, A., and Obermann, W.M. 2003. Aha1 binds to the middle domain of Hsp90, contributes to client protein activation, and stimulates the ATPase activity of the molecular chaperone. *J. Biol. Chem.* **278:** 17228–17235.

Martik, D., Baitinger, C., and Modrich, P. 2004. Differential specificities and simultaneous occupancy of human MutSα nucleotide binding sites. *J. Biol. Chem.* **279:** 28402–28410.

McLaughlin, S.H., Ventouras, L.A., Lobbezoo, B., and Jackson, S.E. 2004. Independent ATPase activity of Hsp90 subunits creates a flexible assembly platform. *J. Mol. Biol.* **344:** 813–826.

Melnick, J., Aviel, S., and Argon, Y. 1992. The endoplasmic reticulum stress protein GRP94, in addition to BiP, associates with unassembled immunoglobulin chains. *J. Biol. Chem.* **267:** 21303–21306.

Melnick, J., Dul, J.L., and Argon, Y. 1994. Sequential interaction of the chaperones BiP and GRP94 with immunoglobulin chains in the endoplasmic reticulum. *Nature* **370:** 373–375.

Meyer, P., Prodromou, C., Hu, B., Vaughan, C., Roe, S.M., Panaretou, B., Piper, P.W., and Pearl, L.H. 2003. Structural and functional analysis of the middle segment of hsp90: Implications for ATP hydrolysis and client protein and cochaperone interactions. *Mol. Cell* **11:** 647–658.

Meyer, P., Prodromou, C., Liao, C., Hu, B., Mark Roe, S., Vaughan, C.K., Vlasic, I., Panaretou, B., Piper, P.W., and Pearl, L.H. 2004. Structural basis for recruitment of the ATPase activator Aha1 to the Hsp90 chaperone machinery. *EMBO J.* **23:** 511–519.

Muresan, Z. and Arvan, P. 1997. Thyroglobulin transport along the secretory pathway. Investigation of the role of molecular chaperone, GRP94, in protein export from the endoplasmic reticulum. *J. Biol. Chem.* **272:** 26095–26102.

Nemoto, T., Matsusaka, T., Ota, M., Takagi, T., Collinge, D.B., and Walther-Larsen, H. 1996. Dimerization characteristics of the 94-kDa glucose-regulated protein. *J. Biochem.* **120:** 249–256.

Nigam, S.K., Goldberg, A.L., Ho, S., Rohde, M.F., Bush, K.T., and Sherman, M. 1994. A set of endoplasmic reticulum proteins possessing properties of molecular chaperones includes Ca(2+)-binding proteins and members of the thioredoxin superfamily. *J. Biol. Chem.* **269:** 1744–1749.

Obermann, W.M., Sondermann, H., Russo, A.A., Pavletich, N.P., and Hartl, F.U. 1998. In vivo function of Hsp90 is dependent on ATP binding and ATP hydrolysis. *J. Cell Biol.* **143:** 901–910.

Panaretou, B., Prodromou, C., Roe, S.M., O'Brien, R., Ladbury, J.E., Piper, P.W., and Pearl, L.H. 1998. ATP binding and hydrolysis are essential to the function of the Hsp90 molecular chaperone in vivo. *EMBO J.* **17:** 4829–4836.

Panaretou, B., Siligardi, G., Meyer, P., Maloney, A., Sullivan, J.K., Singh, S., Millson, S.H., Clarke, P.A., Naaby-Hansen, S., Stein, R., et al. 2002. Activation of the ATPase activity of hsp90 by the stress-regulated cochaperone aha1. *Mol. Cell* **10:** 1307–1318.

Person, M.D., Brown, K.C., Mahrus, S., Craik, C.S., and Burlingame, A.L. 2001. Novel inter-protein cross-link identified in the GGH-ecotin D137Y dimer. *Protein Sci.* **10:** 1549–1562.

Picard, D. 2002. Heat-shock protein 90, a chaperone for folding and regulation. *Cell. Mol. Life Sci.* **59:** 1640–1648.

Pratt, W.B. and Toft, D.O. 2003. Regulation of signaling protein function and trafficking by the hsp90/hsp70-based chaperone machinery. *Exp. Biol. Med. (Maywood)* **228:** 111–133.

Prodromou, C. and Pearl, L.H. 2003. Structure and functional relationships of Hsp90. *Curr. Cancer Drug Targets* **3:** 301–323.

Prodromou, C., Roe, S.M., O'Brien, R., Ladbury, J.E., Piper, P.W., and Pearl, L.H. 1997a. Identification and structural characterization of the ATP/ADP-binding site in the Hsp90 molecular chaperone. *Cell* **90:** 65–75.

Prodromou, C., Roe, S.M., Piper, P.W., and Pearl, L.H. 1997b. A molecular clamp in the crystal structure of the N-terminal domain of the yeast Hsp90 chaperone. *Nat. Struct. Biol.* **4:** 477–482.

Prodromou, C., Panaretou, B., Chohan, S., Siligardi, G., O'Brien, R., Ladbury, J.E., Roe, S.M., Piper, P.W., and Pearl, L.H. 2000. The ATPase cycle of Hsp90 drives a molecular ''clamp'' via transient dimerization of the N-terminal domains. *EMBO J.* **19:** 4383–4392.

Randow, F. and Seed, B. 2001. Endoplasmic reticulum chaperone gp96 is required for innate immunity but not cell viability. *Nat. Cell Biol.* **3:** 891–896.

Richter, K. and Buchner, J. 2001. Hsp90: Chaperoning signal transduction. *J. Cell. Physiol.* **188:** 281–290.

Roe, S.M., Prodromou, C., O'Brien, R., Ladbury, J.E., Piper, P.W., and Pearl, L.H. 1999. Structural basis for inhibition of the Hsp90 molecular chaperone by the antitumor antibiotics radicicol and geldanamycin. *J. Med. Chem.* **42:** 260–266.

Rosser, M.F. and Nicchitta, C.V. 2000. Ligand interactions in the adenosine nucleotide-binding domain of the Hsp90 chaperone, GRP94. I. Evidence for allosteric regulation of ligand binding. *J. Biol. Chem.* **275:** 22798–22805.

Rosser, M.F., Trotta, B.M., Marshall, M.R., Berwin, B., and Nicchitta, C.V. 2004. Adenosine nucleotides and the regulation of GRP94-client protein interactions. *Biochemistry* **43:** 8835–8845.

Sinz, A. 2003. Chemical cross-linking and mass spectrometry for mapping three-dimensional structures of proteins and protein complexes. *J. Mass Spectrom.* **38:** 1225–1237.

Soldano, K.L., Jivan, A., Nicchitta, C.V., and Gewirth, D.T. 2003. Structure of the N-terminal domain of GRP94. Basis for ligand specificity and regulation. *J. Biol. Chem.* **278:** 48330–48338.

Stebbins, C.E., Russo, A.A., Schneider, C., Rosen, N., Hartl, F.U., and Pavletich, N.P. 1997. Crystal structure of an Hsp90-geldanamycin complex: Targeting of a protein chaperone by an antitumor agent. *Cell* **89:** 239–250.

Wearsch, P.A. and Nicchitta, C.V. 1996. Endoplasmic reticulum chaperone GRP94 subunit assembly is regulated through a defined oligomerization domain. *Biochemistry* **35:** 16760–16769.

Wegele, H., Muschler, P., Bunck, M., Reinstein, J., and Buchner, J. 2003. Dissection of the contribution of individual domains to the ATPase mechanism of Hsp90. *J. Biol. Chem.* **278:** 39303–39310.

Wegele, H., Muller, L., and Buchner, J. 2004. Hsp70 and Hsp90—A relay team for protein folding. *Rev. Physiol. Biochem. Pharmacol.* **151:** 1–44.

Whitesell, L. and Lindquist, S.L. 2005. HSP90 and the chaperoning of cancer. *Nat. Rev. Cancer* **5:** 761–772.

Yamada, S., Ono, T., Mizuno, A., and Nemoto, T.K. 2003. A hydrophobic segment within the C-terminal domain is essential for both client-binding and dimer formation of the HSP90-family molecular chaperone. *Eur. J. Biochem.* **270:** 146–154.

Young, M.M., Tang, N., Hempel, J.C., Oshiro, C.M., Taylor, E.W., Kuntz, I.D., Gibson, B.W., and Dollinger, G. 2000. High throughput protein fold identification by using experimental constraints derived from intramolecular cross-links and mass spectrometry. *Proc. Natl. Acad. Sci.* **97:** 5802–5806.

Zhao, R., Davey, M., Hsu, Y.C., Kaplanek, P., Tong, A., Parsons, A.B., Krogan, N., Cagney, G., Mai, D., Greenblatt, J., et al. 2005. Navigating the chaperone network: An integrative map of physical and genetic interactions mediated by the hsp90 chaperone. *Cell* **120:** 715–727.